Simulation studies of pore and domain formation in a phospholipid monolayer

Volker Knecht, Michiel Müller, Mischa Bonn, Siewert-Jan Marrink, and Alan E. Mark

Citation: The Journal of Chemical Physics **122**, 024704 (2005); doi: 10.1063/1.1825992
View online: http://dx.doi.org/10.1063/1.1825992
View Table of Contents: http://scitation.aip.org/content/aip/journal/jcp/122/2?ver=pdfcov
Published by the AIP Publishing

Simulation studies of pore and domain formation in a phospholipid monolayer

Volker Knecht[a)]
Department of Biophysical Chemistry, University of Groningen, Nijenborgh 4, 9747 AG Groningen, The Netherlands

Michiel Müller
Swammerdam Institute for Life Sciences, University of Amsterdam, P.O. Box 94062 1090 GB Amsterdam, The Netherlands

Mischa Bonn
Leiden Institute of Chemistry, P.O. Box 9502, 2300 RA Leiden, The Netherlands; FOM-Institute for Atomic and Molecular Physics AMOLF, Kruislaan 407, 1098 SJ Amsterdam, The Netherlands

Siewert-Jan Marrink and Alan E. Mark
Department of Biophysical Chemistry, University of Groningen, Nijenborgh 4, 9747 AG Groningen, The Netherlands

(Received 21 July 2004; accepted 8 October 2004; published online 17 December 2004)

Despite extensive study the phase behavior of phospholipid monolayers at an air–water interface is still not fully understood. In particular recent vibrational sum-frequency generation (VSFG) spectra of DPPC monolayers as a function of area density show a sharp transition in the order of the lipid chains at 1.10 nm^2/molecule. This is in a region where the lateral pressure as a function of area is effectively constant. We have investigated the nature of this transition by studying the phase behavior of DPPC monolayers as a function of area density using molecular-dynamics simulations. The changes in order within the monolayer as a function of area density correlate well with the experimental signal. At 0.58 nm^2/molecule we observe the onset of lateral separation of highly ordered and disordered lipids, indicating the coexistence of a gel-like liquid condensed and a fluidlike liquid expanded phase. At 0.97 nm^2/molecule the monolayer ruptures, marking the onset of the liquid–gas (G) coexistence region. This is much earlier than suggested by fluorescence microscopy results and implies that at the point of rupture, the initial pores have an equilibrium size smaller than ~500 nm in diameter. The rupture of the monolayer leads to a sharp increase in the overall lipid order that explains the sharp transition observed in the VSFG measurements. VSFG measurements thus may represent a sensitive means to determine the onset of the liquid–gas (G) coexistence region for such systems.
[DOI: 10.1063/1.1825992]

INTRODUCTION

Monomolecular layers at an air–water interface are a well-studied example of a self-organized system.[1] Understanding their behavior is essential for the Langmuir–Blodgett technique which involves the formation of a monolayer film on a water surface with subsequent transfer onto a solid substrate.[2] In a biological context phospholipid monolayers are a model system for membrane biophysics, as a lipid bilayer, the basis for a biological membrane, can be considered as two weakly coupled monolayers.[3] Phospholipid monolayers are also used as a model for lung surfactant, a complex mixture of lipid and protein that has been proposed to form a monolayer at the alveolar liquid–air interface.[4] Lung surfactant modulates the surface tension of the lung, stabilizing alveoli against collapse during expiration and minimizing the work required to expand the alveoli again during inhalation.[5] The major component (>90%) of lung surfactant is phospholipid. The predominant species is DPPC (dipalmitoylphosphatidylcholine) which ranges from 40% to 80% by weight in natural surfactant.[4] During breathing the lateral pressure on the alveolar surface varies substantially. How phospholipid monolayers respond to large changes in area per lipid is not fully understood.[1]

Figure 1 shows a plot of the area per lipid versus the lateral pressure for DPPC monolayers at an air–water interface at a temperature of ~290 K.[6] The existence of several distinct phases[1] is evident: At high compression (molecular area $A<0.47\,nm^2$) the monolayer is in a condensed[3] (*C*, historically termed *solid condensed*[1]) phase. Here the lipid chains are in an all-trans conformation[3] and aligned parallel to each other.[1] The lipid chains tilt such that the projected area of the hydrocarbon chains in the plane parallel to the water surface matches that of the headgroups.[5] Upon decompression ($A>0.47\,nm^2$) the *C* phase coexists[7] with a gel-like[8] liquid condensed (LC) phase[7] in which lipid chains have gauche defects[3] but are still aligned.[1] Between 0.50 and 0.80 nm^2/molecule the LC phase coexists with a more disor-

[a)]Author to whom correspondence should be addressed. Electronic mail: address: v.knecht@chem.rug.nl

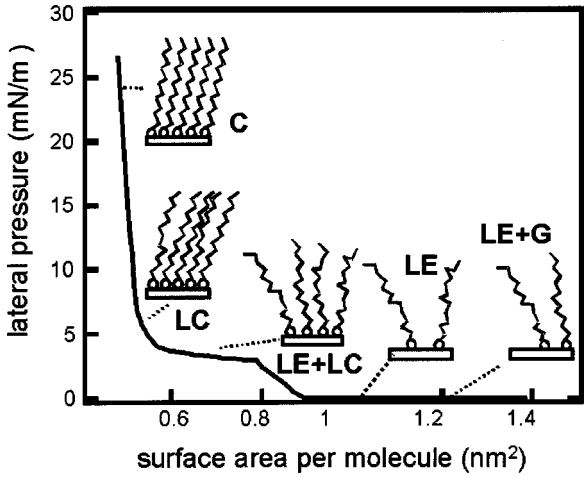

FIG. 1. Phase diagram of a DPPC monolayer at ~290 K (modified from Ref. 3) showing the condensed (C), liquid condensed (LC), liquid-condensed–liquid expanded (LE) coexistence region, the LE phase, and the liquid expanded–gas (LE+G) coexistence region.

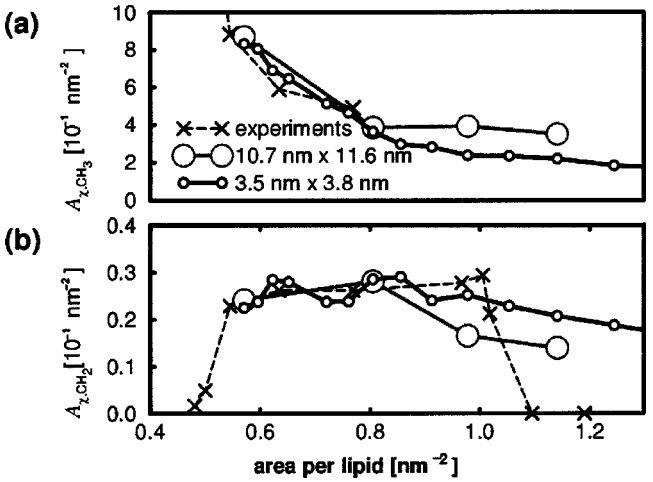

FIG. 2. Nonlinear susceptibilities of the CH_3 (a) and CH_2 (b) bond stretch vibrations from experiment (Ref. 3) (*crosses*) and calculated from the simulations according to Eq. (3) for small (lateral dimensions 3.5 nm×3.8 nm, *small circles*) and large (lateral dimensions 10.7 nm×11.6 nm, *large circles*) monolayer patches at different areas per molecule are shown. The susceptibilities from experiment (given only in arbitrary units) were scaled such that the values lay in the same range as those from the simulations.

dered and fluidlike[8] liquid expanded (LE) phase in which lipid tails are no longer aligned and are highly disordered.[6] Between 1.0 and 4.0 nm^2/molecule, a region in which the lateral pressure is effectively zero,[9] the LE phase is believed to coexist with a gas (G) phase[3,9] in which the lipid tails have substantial contact with the water surface, but little with each other.[5]

Fluorescence microscopy has revealed that in the liquid (L)-gas coexistence region of DPPC monolayers at small gas phase fractions the gas phase is present as holes [two-dimensional (2D) gas bubbles[10]] in an interconnected liquid phase[9] such that the monolayer forms a two-dimensional foam.[11] However, due to the limited spatial resolution of fluorescence microscopy images[9] the precise onset of the L–G coexistence region cannot be determined directly using fluorescence microscopy. Furthermore, neither the lateral pressure nor the surface potential can be determined with sufficient accuracy[12] to precisely determine onset of the L–G coexistence region leading to considerable uncertainty in this quantity.

Recently, a sharp transition of unknown nature at 1.1 nm^2/molecule has been detected using vibrational sum frequency generation (VSFG) measurements.[3] The VSFG effect arises when two applied electromagnetic fields of different frequencies in the form of an infrared and a visible laser pulse interact with vibrational modes of the medium and induce an electromagnetic field whose frequency is the sum of those of the incoming fields.[13] This second-order nonlinear process is surface-sensitive. It is forbidden in a medium with inversion symmetry while allowed at an interface where the inversion symmetry is broken. The resulting spectra show resonances at characteristic vibrational frequencies of the medium and thus are capable of selective detection of vibrations of surface molecules.[14] As the resonance intensity is proportional to the average component of the respective transition dipole moment vector normal to the interface, VSFG measurements are sensitive to the ordering of functional groups.

In VSFG measurements of fully compressed DPPC monolayers resonances from symmetric and asymmetric bond stretching modes of the terminal methyl (CH_3) groups of the alkyl chains show a strong signal, indicating strong ordering of the lipid tails. On increasing the area per molecule the signal rapidly decreased [see Fig. 2(a) *crosses*], indicating a loss of order upon expansion. In contrast the bond stretching modes of methylene (CH_2) groups of the lipid alkyl chains give no signal in the fully compressed monolayer due to inversion symmetry arising from the all-trans configuration of the lipid tails. Upon increasing the area per lipid the CH_2 signal increases rapidly [Fig. 2(b) *crosses*], indicating a break in inversion symmetry most likely due to the appearance of gauche defects. Between 0.55 nm^2/molecule and 1.10 nm^2/molecule the signal is constant. In this region the decrease of inversion symmetry due to increasing number of gauche defects, the decrease in order normal to the interface and the decrease in lipid density counterbalance each other. At 1.10 nm^2/molecule the CH_2 signal suddenly disappears. This has been interpreted by some as a sudden transition from an ordered to a disordered state of the lipids and attributed to a co-operative curling of the lipid molecules.[3] Roke *et al.*[3] argued that the sharp transition observed by VSFG could not be the LE–G transition. This is because the LE–G transition exhibits a large coexistence region (i.e., it is noncooperative and initially only affects a small fraction of molecules), whereas VSFG is a general probe with low spatial resolution.

The curling hypothesis, however, is questionable for two reasons: (1) The proposed curling transition would require a co-operative disassembly of the lipid aggregates[3] and thus would essentially correspond to a liquid–gas transition. However, the liquid–gas transition of DPPC monolayers is not believed to be cooperative. (2) The energetics of the absorption of the alkyl chains of fatty acids at very low concentration suggest that the tails of lipids in the gas phase lie extended on the surface and are not curled.[15] Thus, although

the sudden disappearance of the VSFG resonances might indicate a phase transition, the origin of this transition is unclear. As the VSFG signal is an integrated quantity dependent on the lipid density, the degree to which inversion symmetry is broken and on the ordering normal to the interface, the behavior of the VSFG signal as a function of the area per lipid is difficult to interpret.

In this work we have used molecular-dynamics (MD) simulations[16] in order to investigate the nature of the structural changes associated with changes in lipid density. To compare the results of the simulations to the available experimental data the trajectories were used to back-calculate the VSFG signal.

The structure and dynamics of monolayers have been examined in a number of previous simulation studies. These are reviewed in Ref. 1. In particular, Okamura *et al.* obtained direct correlation with experiment by calculating infrared spectra of monolayers of stearic acid as a function of area density.[17] In simulations by Tomassone *et al.* using a coarse-grained model of soluble surfactants the G–LE coexistence region at low area densities was reproduced.[18] In more recent work monolayers comprising DPPC mixed with an anionic lipid[19] as well as monolayers containing a human surfactant protein[20] were simulated to study pulmonary surfactant-associated phenomena. The coexistence of multiple lipid phases, however, which is essential for determining the phase diagram of phospholipid monolayers, has to our knowledge not previously been studied using atomistic simulations.

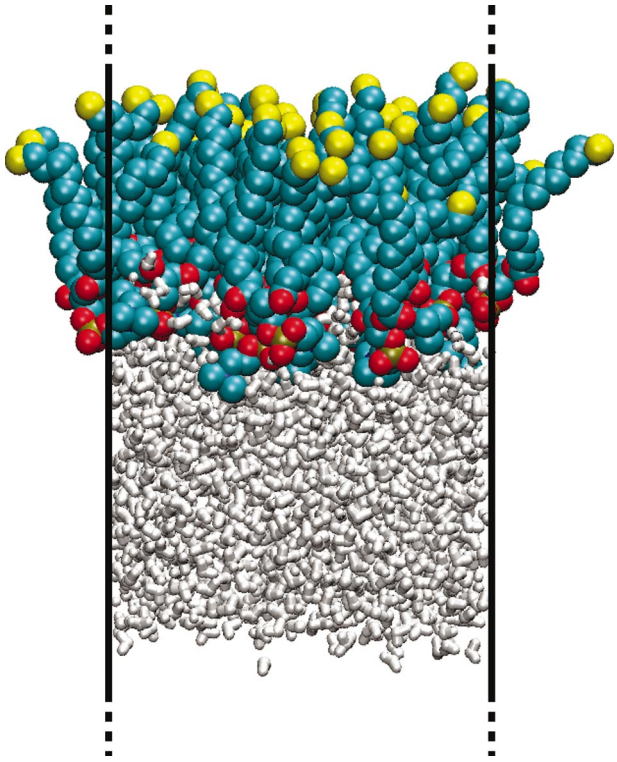

FIG. 3. (Color) Small simulation system (dimensions 3.5 nm×3.8 nm) at 0.57 nm^2/molecule. Water molecules are shown in white. DPPC lipids are colored according to the atom types (carbon in cyan, phosphate in brown, oxygen in red, nitrogen in blue; hydrogen atoms of aliphatic groups were not simulated explicitly, but described using united atoms). The carbon atoms at the termini of the lipid tails are highlighted in yellow.

METHODS

Simulations

The system used in this work was simulated under two-dimensional periodic boundary conditions and is shown in Fig. 3. The system consisted of a monolayer of DPPC on a slab of 1321 water molecules. The initial configuration of the system was derived from an equilibrated bilayer in water. The single monolayer was generated by removing the second monolayer and extending the box in the direction perpendicular to the monolayer until the system was effectively only periodic in the plane of the monolayer. The monolayer was comprised of 24 lipid molecules. The simulations were carried out at constant volume with the lateral dimensions being 3.5 nm×3.8 nm. In the direction normal to the interface (z axis) vacuum boundary conditions were achieved by setting the box dimension to a value of 20 nm. During the simulations water molecules enter the vacuum region, but due to the finite size of the system re-enter the lipid–water phase. On average only a few water molecules reside in the vacuum region. The area per lipid was varied between 0.57 and 1.37 nm^2 by removing lipid molecules. Each system was simulated for 8 ns.

A curled lipid was modeled by simulating a single lipid molecule in vacuum, starting from a configuration of a lipid taken from an equilibrated bilayer. In this vacuum simulation position restraints were imposed on the atoms of the headgroup. The configuration of the lipid molecule after 8 ns was taken as the initial configuration of a curled lipid molecule at an air–water interface. The single lipid was placed onto a water slab and all water molecules that overlapped with the lipid removed to generate the interface. The system was then energy-minimized and the water slab was equilibrated for 8 ns with position restraints on the lipid atoms. In the subsequent 8 ns simulation the lipid was allowed to move freely.

To study finite size effects, a ninefold larger patch of a DPPC monolayer at an air–water interface was simulated at areas corresponding to 0.57, 0.97, 1.05, and 1.14 nm^2/molecule. The initial structures were obtained from the final structures of the simulations of respective small patches by reducing the number of water molecules to 760 and copying the system to a 3×3 array. This resulted in systems with lateral dimensions of 10.7 nm×11.6 nm, comprising between 108 and 216 lipids together with 6849 water molecules. These larger systems were simulated for 23 ns each.

All simulations were performed using the GROMACS[21] simulation suite. The DPPC molecules were described using the force field of Berger *et al.*[22] in which the nonpolar hydrogen atoms of the lipids are described using united atoms. The water molecules were described using the SPC model.[23] The covalent bond lengths in the lipid and water molecules were constrained using the LINCS and SETTLE methods, respectively.[24,25] In addition the total mass of the molecule was redistributed in order to increase the mass of the hydrogen atoms. Together this allowed the use of a time step of 4 fs.[26] The temperature was kept constant at 293 K, the temperature at which the new phase was detected.[3] This was

achieved by separately coupling the lipids and water to an external temperature bath using a Berendsen thermostat.[27] The coupling constant was 0.1 ps. Lennard-Jones and electrostatic interactions within a cut-off 1.4 nm were evaluated every time step. The neighbor list was updated every ten steps. A reaction field[28] with a dielectric constant $\epsilon_r = 54$ was used to correct for the neglect of electrostatic interactions beyond the cutoff. The simulation conditions used have been well tested in previous simulations of bilayer systems (setup K1 in Ref. 29). Snapshots were saved every 40 ps for analysis.

General analysis

The simulations of the small and large monolayer patches were analyzed omitting the initial 3 and 17 ns, respectively, for equilibration. The ordering of the lipid tails at each of the CH_2 carbons C_n was monitored by determining the $S_{z,n}$ order parameters where

$$S_{z,n} = \tfrac{3}{2}\langle \cos^2 \theta_{z,n}\rangle - \tfrac{1}{2}. \quad (1)$$

Here $\theta_{z,n}$ denotes the angle between the normal of the interface (z axis) and the molecular axis defined by the vectors connecting the carbon atoms C_{n+1} and C_{n-1}. Values of S_z larger than zero indicate that the segments are preferentially oriented normal to the interface. Smaller than zero indicates an orientation in the plane of the interface and zero would correspond to an isotropic orientation.

The association between the lipids was analyzed by determining the pair correlation function between the phosphate atoms of the lipid headgroups. The pair correlation functions were obtained by dividing the distance scale into intervals of 0.02 nm. The correlation functions were smoothed using a Gaussian filter of width 0.04 nm and normalized to the total number of lipids in the system.

Calculation of VSFG signal

In order to be able to directly relate the results from the simulations to the VSFG data obtained experimentally, the nonlinear susceptibility was calculated from the simulations. The nonlinear susceptibility $\chi^{(2)}$ is a third-rank tensor defined as[14]

$$P_i^{(2)}(\omega_1+\omega_2) = \sum_{j,k} \chi_{ijk}^{(2)}(\omega_1+\omega_2) E_j(\omega_1) E_k(\omega_2), \quad (2)$$

where $\mathbf{P}^{(2)}(\omega_1+\omega_2)$ is the sum-frequency polarization per unit volume induced by two incoming fields $\mathbf{E}$ of frequencies ω_1 and ω_2. In the experiments the polarizations of the in- and out-coming fields were chosen so as to probe the components $\chi_{xxz}^{(2)} = \chi_{yyz}^{(2)} \equiv \chi$.[3,13] These components were also investigated in the simulations.

We assume that the third-rank second-order nonlinear polarization tensor α[13] of each of the methyl and methylene groups is dominated by a single component, i.e., that the second-order polarization of these groups only occurs along a single direction given by a polarization vector $\vec{\mu}$. For the CH_2 signal $\vec{\mu}$ points along the bisector of the two corresponding C–H bond vectors (as hydrogen atoms were not simulated explicitly, $\vec{\mu}$ was constructed from the positions of the carbon atoms assuming an ideal tetrahedral geometry). For the CH_3 signal the polarization vector points along the terminal C–C bond of the alkyl chain. Denoting θ_{CH_i} as the angle between the z axis and the respective polarization vector and neglecting terms $\mathcal{O}(\cos^3 \theta_{CH_i})$ yields[30]

$$\chi_{CH_i} \propto N_L \langle \cos \theta_{CH_i}\rangle \equiv A_{\chi,CH_i} \quad i = 2,3. \quad (3)$$

Here N_L denotes the number of lipid molecules per area. Note that this term is also sensitive to the symmetry of the lipid chain conformation: For an all-trans conformation the contributions of adjacent methylene groups in the lipid chain have opposite signs and thus cancel on average. Methylene groups yield no net contribution unless the inversion symmetry is broken due to the presence of gauche defects.

In Eq. (3) only the CH_2 and CH_3 groups of the tails were considered. There are two experimental indications for assuming that the headgroup CH_2 and CH_3 groups do not contribute significantly to the VSFG signal: (1) In experiments with DPPC deuterated at the alkyl chains (D62-DPPC) no VSFG signal in the C–H stretching region was detected. (2) No CH_2 signal is seen for a completely ordered layer. Note, because the symmetry argument applies only to the alkyl chain, the headgroup CH_2 groups could in principle give rise to a signal. Possible reasons why no signal is observed include (i) a very small Raman/IR cross section or (ii) the resonance may be shifted. Most likely, however, the CH_2 groups in the headgroups are simply highly disordered. For the same reason, no contribution from the CH_3 groups in the headgroups is expected as these groups are not expected to be well-ordered (even at complete compression).

Fluorescence microscopy

Fluorescence microscopy was used to study domain formation in a DPPC monolayer at molecular areas between 0.55 and 1.6 nm^2. DPPC was obtained from Avanti Polar Lipids (Birmingham, Alabama), the fluorescent probe, Rh-PE (rhodamine B 1,2-dihexadecanoyl-*sn*-glycero-3-phosphoethanolamine, triethylammonium salt) from Molecular Probes. The fluorescence experiments were carried out by spreading the phospholipid from a 1 mg/ml solution in chloroform, with a probe concentration of 1 mol%, onto Millipore water (18.2 $M\Omega\,cm$ resistivity) at pH 7, in a commercial, motorized Teflon trough from Kibron, Inc. Fluorescence images were taken with a CoolSnap fix CCD camera (Photometrics) mounted on an Olympus BX-60 fluorescence microscope, with an Olympus 20×/0.55 NA achromat microscope objective with a ~0.5 μm resolution.

RESULTS

Curling hypothesis

Figure 4 shows snapshots of the small DPPC monolayer patches simulated at various areas per molecule after 6 ns of simulation. From Fig. 4(a) it can be seen that at 0.57 nm^2/molecule most lipid alkyl chains are either in an all-trans conformation or have gauche defects which do not perturb significantly the overall ordering normal to the interface. Figures 4(b) and 4(c) show that expanding of the monolayer

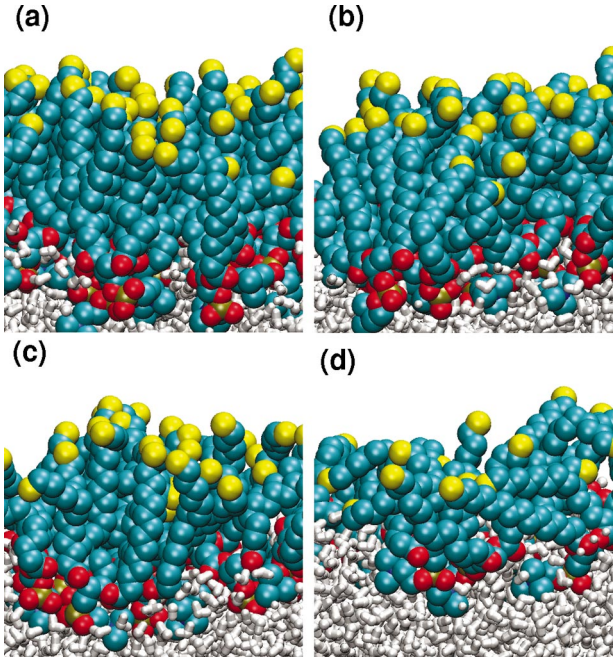

FIG. 4. (Color) Snapshots after 6 ns of simulations of the small DPPC monolayer patches (dimensions 3.5 nm×3.8 nm) with molecular areas of 0.57 nm^2 [LC–LE coexistence region with a large LC phase fraction, (a)] and 0.65 nm^2 [LC–LE coexistence region with intermediate LC phase fraction, (b)], 0.76 nm^2 [LC–LE coexistence region with low LC phase fraction, (c)] and 1.37 nm^2 [new phase, (d)]. The color scheme is as in Fig. 3.

to 0.65 nm^2/molecule and 0.76 nm^2/molecule, respectively, progressively decreases the lipid ordering. Figure 4(d) shows the monolayer at 1.37 nm^2/molecule which is well within the proposed ''curling'' phase ($A > 1.10\,nm^2$/molecule). The lipid tails become more disordered and are inhomogeneously distributed in the interface. For a large fraction of the time the chains lie flat on the water surface. Some tails show strong kinks, but overall they remain spatially extended and do not curl.

Figure 5(a) shows a top view of a larger monolayer patch at 0.57 nm^2/molecule. The white circle marks a domain in which the chains are tightly packed in a hexagonal lattice, indicating a LC domain. Figures 5(b) and 5(c) show side views of the same configuration. The LC domain is shown on the left side of Figs. 5(b) and 5(c). It can be seen that here the lipid tails are fully extended and have only few gauche defects. As a result, in the LC domain the monolayer is thicker than in the remaining part of the monolayer. All these observations are in accordance with the literature.[1,3,5]

As an additional test a single lipid was placed at an air–water interface in a curled conformation. It was found that the lipid uncurled within 120 ps and remained uncurled during the subsequent 7.9 ns of simulation. A curled conformation is expected to be unfavorable due to a partial dehydration of the headgroup. The simulations demonstrate that a curled lipid conformation is not stable at an air–water interface, implying the observed transition must have a different origin.

Lipid order

The simulations do, nevertheless, show a sharp change in lipid order around 1.0 nm^2/molecule. Figure 6(a) shows

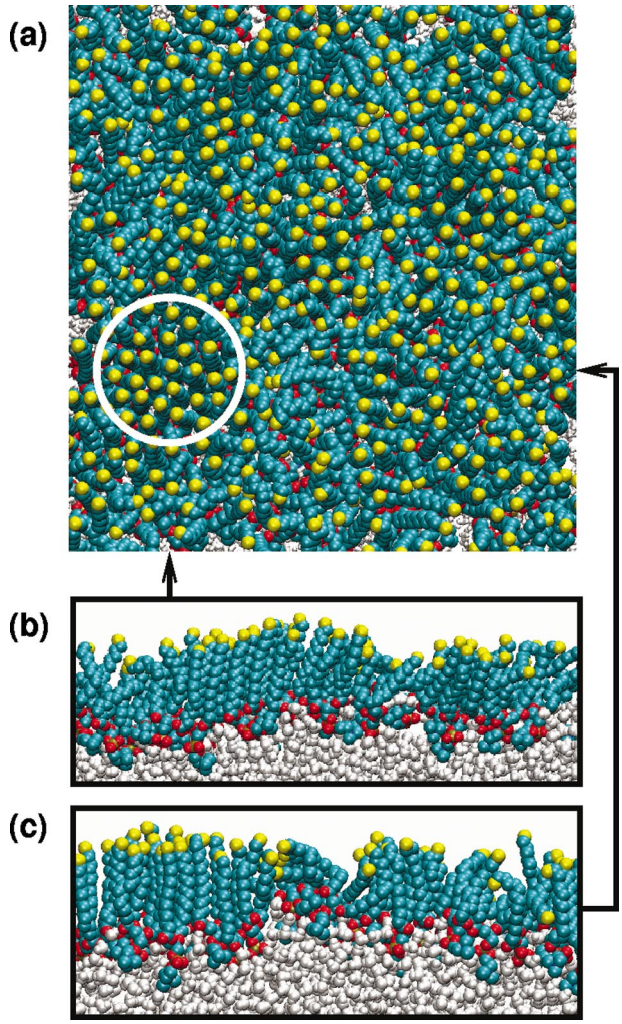

FIG. 5. (Color) Larger monolayer patch (dimensions 10.7 nm×11.6 nm) in the LC–LE coexistence region (0.57 nm^2/molecule) after 7.8 ns of simulation. (a) View from the air phase. The white circle marks a LC domain, indicated by a hexagonal arrangement of the terminal carbon atoms of lipid tails (*yellow*). (b) and (c): Side views of slices along the straight lines indicated by the arrows. The color scheme is as in Fig. 3.

the order parameters of the tail segments for three different areas per molecule. At 0.57 nm^2/molecule (*diamonds*) all tail segments orient normal to the interface. The order is highest close to the headgroup and decreases slightly toward the termini of the tails.

In the simulations of a single lipid, corresponding to a monolayer at infinite dilution, i.e., in the gas phase [Fig. 6(a) *circles*], the order is dramatically reduced. Only the first three tail segments close to the headgroup are still ordered normal to the interface. This residual order is presumably due to the strong hydration of the headgroup drawing the lipid into the water phase. Overall the tail is oriented in the plane of the interface as has already been inferred from studies of the energetics of absorption to the interface for alkyl chains of fatty acids at very dilute solutions.[15]

At 1.37 nm^2/molecule [Fig. 6(a) *squares*] the order is higher than that found for an isolated lipid, but still the majority of segments show no ordering normal to the interface (isotropic). As there is little ordering of the C–H bonds the VSFG signal [see Eq. (3)] would be expected to be low as is

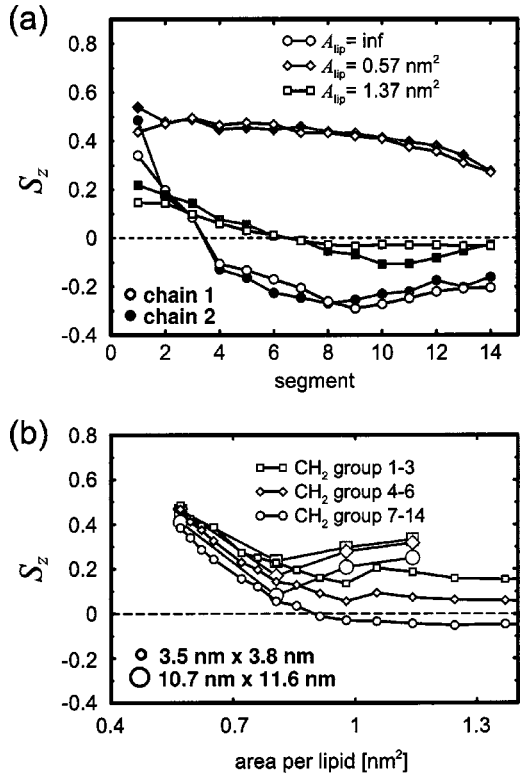

FIG. 6. Order parameters S_z from Eq. (1) for the CH_2 groups of the lipid chains. (a) Order parameters for small monolayer patches (lateral dimensions 3.5 nm×3.8 nm) for three different areas per lipid molecule for chain 1 (*open symbols*) and chain 2 (*filled symbols*). (b) Order parameters of groups of tail segments as a function of the area per lipid molecule for the small (*small symbols*) and large (lateral dimensions 10.7 nm×11.6 nm, *large symbols*) systems simulated. The numbering of the tail segments starts from the headgroup.

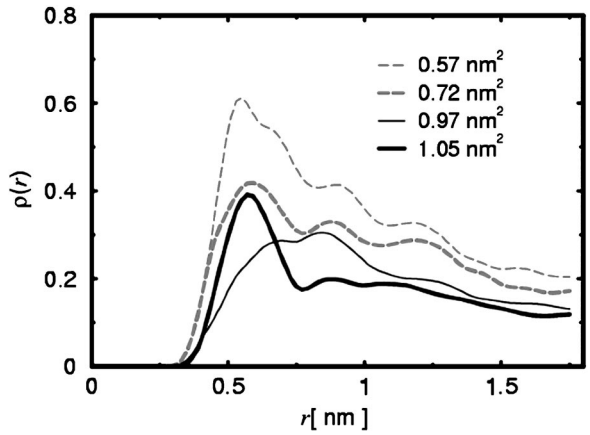

FIG. 7. Pair correlation functions for phosphate atoms for different areas per molecule from simulations of small monolayer patches (lateral dimensions 3.5 nm×3.8 nm). The normalization is chosen such that the integral of each correlation function is the total number of lipid molecules in the simulation system.

observed. Plotting the order parameters as a function of area per lipid [Fig. 6(b)] shows, however, that the off- to in-plane transition of the terminal tail segments is a *smooth* transition. It is unlikely that this is related to the sharp transition observed in the VSFG experiments. A small but sharp transition, however, does occur at 1.05 nm^2/molecule in the small systems. At this molecular area the order of the tail segments closest to the headgroup suddenly *increases*.

The increase in the tail order suggests that adjacent lipids bind more strongly to each other. Pair correlation functions for the phosphate atoms of the lipids (see Fig. 7) show that this is indeed the case. At 0.57 nm^2, corresponding to the LC–LE coexistence region with a large LC component, the first neighbor peak has a sharp component for small distances and a shoulder for larger distances. This can be interpreted as an overlap of a sharp peak reflecting the dominant LC phase and a broad peak reflecting the LE component. Increasing the area to 0.72 nm^2 increases the LE component and makes it the dominant phase; the LC phase is only visible as a small shoulder at short distances. At 0.97 nm^2/molecule the first neighbor peak is shifted toward larger distances and becomes smaller than the second neighbor peak, indicating that the monolayer is under tension.

Figure 8(c) shows that at an area of ~0.98 nm^2/molecule holes begin to form in the monolayer. During the simulations pores transiently open and close. However, at ~1.05 nm^2/molecule [Fig. 8(d)] the monolayer ruptures and a stable pore is formed. Hence at this area the system is in the liquid–gas phase coexistence region. The partial rupture of the monolayer releases the stress in the monolayer and the phosphate groups can again bind strongly to their first neighbors (Fig. 7, *black solid curve*) as in the LE phase. The stronger lipid binding explains the increased ordering of the lipid tails [Fig. 6(b) *small symbols*].

The sharpness of the transition is related to the size of the simulated system. From the simulations of the larger sys-

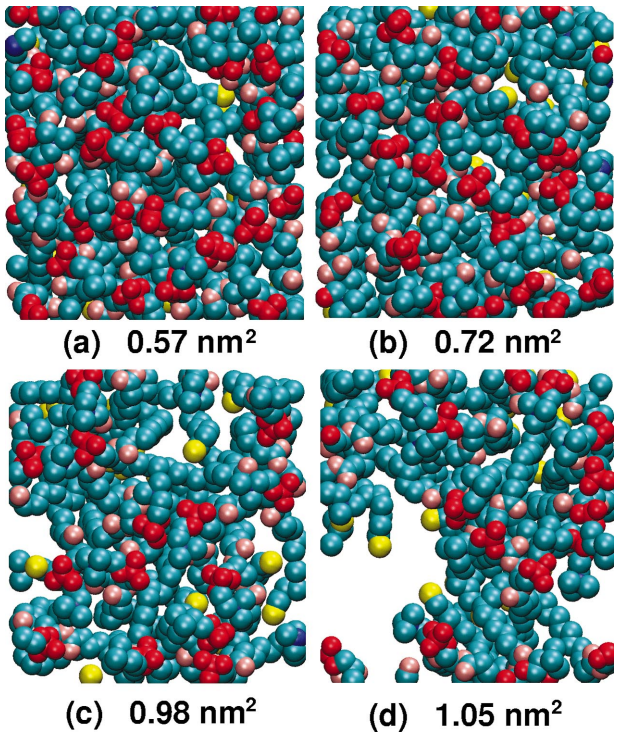

FIG. 8. (Color) Snapshots after 6 ns of simulations of DPPC monolayer patches (lateral dimensions 3.5 nm×3.8 nm) at various areas per molecule viewed from the water phase. The color scheme is similar to Fig. 3. Note, phosphate groups are highlighted in red for comparison to Fig. 7. Carbonyl oxygen atoms are shown in pink.

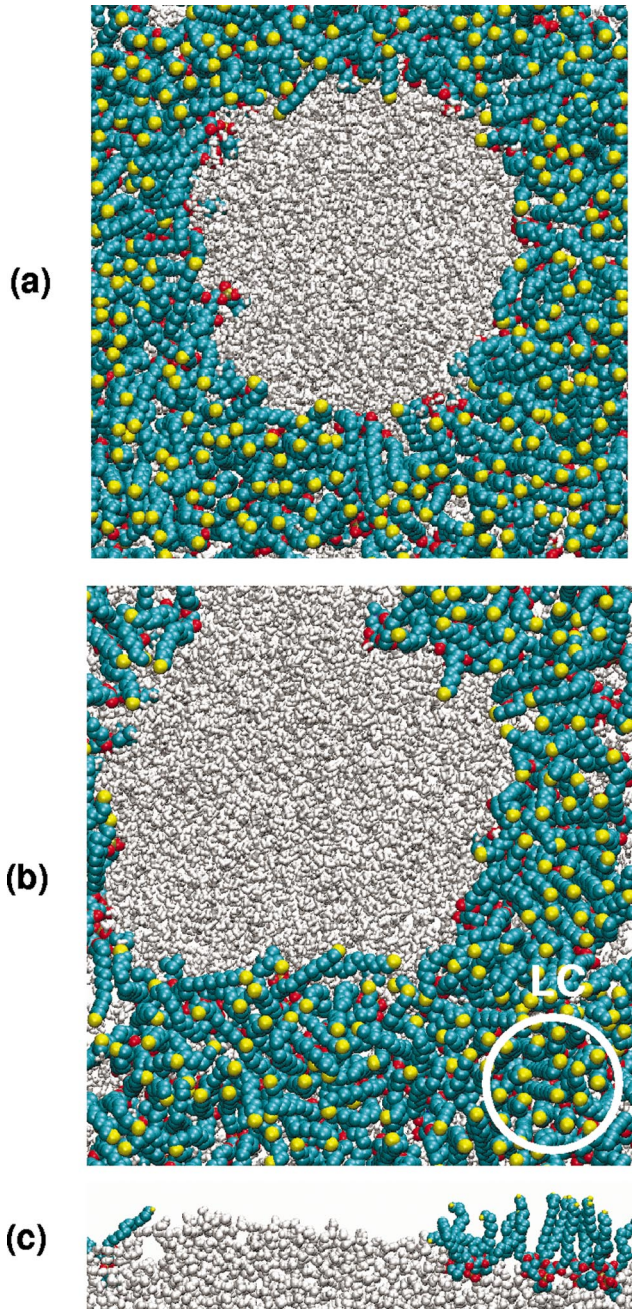

FIG. 9. (Color) Snapshots of DPPC monolayer patches (dimensions 10.7 nm×11.6 nm) at 0.97 (a) and 1.14 nm^2/molecule (b) after 20 ns of simulation viewed from the air phase. For the configuration shown in (b) a slice (along the diagonal from the upper left to the lower right) is also shown (c). The color scheme is as in Fig. 3.

tem it can be seen that in the LC–LE coexistence region (molecular areas 0.57 and 0.80 nm^2) the size of the system has little effect in terms of the overall lipid order [Fig. 6(b) *large symbols*]. However, the rupture of the monolayer occurs at a smaller molecular area of 0.97 nm^2 [Fig. 9(a)] and as shown in Fig. 6(b) (*large symbols*) the rupture induces a stronger increase of the overall order than for the small system (*small symbols*). In fact the lipids become even more strongly ordered than in the fully expanded monolayer (0.80 nm^2/molecule).

The finite-size effects on the overall lipid order arise from the fact that (1) lipids at the pore boundary have lower order than lipids in the bulk [see Fig. 9(c)] and (2) the size of the system simulated limits the size of the pore. In the larger system the small pores from the initial configuration assembled to a single large pore [Fig. 9(b)] within 16 ns. The larger pore implies a larger ratio of bulk versus boundary lipids and hence higher lipid order overall.

Ruptured monolayer

The formation of a pore marks the beginning of the liquid–gas coexistence region of the monolayer. In the pores the water level was elevated associated with a lifting of lipid head-groups at the pore boundary [Fig. 9(c)]. In previous molecular-dynamics simulations of lipid bilayers water pores induced by applying lateral tension[31] were also found to be lined by lipid headgroups.

At the edges of the pore the lipid tails are highly disordered. However, as seen in Figs. 9(b) (*lower right*), and 9(c) (*right*), away from the edge of the pore highly ordered domains can form in which the lipid tails have few gauche defects, are aligned and are tightly packed, all characteristic of a LC domain. In the rest of the system lipids show intermediate order, characteristic of the LE phase.

Fluorescence microscopy images of DPPC monolayers at the smallest areas per lipid at which a gas–liquid coexistence can be detected by this technique show the presence of micrometer sized pores in an interconnected liquid phase.[9] The structure observed in the simulations is similar to that observed in the micrographs although the size of the initial pores in the simulations is ~3 orders of magnitude smaller. The size of the pores that are observed experimentally are correlated with the area fraction of the gas phase.[9,10] They are also related to the quality of the fluorescence images which were limited to micron resolution.

In order to determine what was the upper limit of the possible pore size a series of fluorescence microscopy images were obtained with sub-micron resolution. It was first verified that at the fluorophore concentration used there was no significant change in the DPPC pressure-area isotherm. The isotherms with and without fluorophore were essentially identical, apart from a very small variation in the tilt of the LE–LC coexistence plateau for the DPPC/Rh-PE fluorophore-mixture relative to the pure DPPC monolayer system. In these images LE domains appear as brightly fluorescent regions, LC and gas domains appear as dark regions.[3,9] As in previous experiments[3] we observed domain formation associated with LE–LC coexistence at a surface area per DPPC molecule between 0.55 and 0.88 nm^2. No domain formation was observed at areas between 0.88 and 1.6 nm^2 per molecule. This implies that if pores are present in this range of area density they must be smaller than ~500 nm in diameter. Unfortunately, it is not possible to estimate what would be the equilibrium size of a pore expected in this region from the simulations. The size of the pore (~7.0 nm in diameter at 1.14 nm^2/molecule) is limited by the size of the system and thus only represents a lower bound for pores that form at the onset of the L–G coexistence region in expanded systems.

Simulated VSFG signals

To demonstrate that the simulations are in fact consistent with the VSFG experiments, second-order nonlinear susceptibilities for the CH_2 and CH_3 bond stretching modes were determined using Eq. (3). In Fig. 2(a) are plotted the calculated susceptibilities as a function of the area per lipid. From Fig. 2(a) it can be seen that with increasing area per molecule the CH_3 signal from the small monolayer patches (*small circles*) decreases gradually. The decrease is both due to the decreased lipid density and a decreased ordering of the terminal C–C bonds normal to the interface.

Between 0.57 and 1.05 nm^2 the CH_2 signal [Fig. 2(b), *small circles*] shows only small variations, indicating that the decrease in lipid density N_L [Eq. (3)] is counterbalanced by an increase in net polarization $\langle \cos \theta_{CH_2} \rangle$ of the CH_2 groups. The signal here is in line with the experimentally observed plateau in this region [Fig. 2(b) *crosses*].[3] Note, the susceptibilities determined from experiment were given only in arbitrary units. The experimental values were scaled by a uniform factor such that the values lay in the same range as those from the simulations. In principle, to reproduce the experimental signal correctly one would require an equilibrium distribution of LC and LE domain sizes. It is known from fluorescence microscopy[3] that the size of these domains is in the μm range. The required system sizes and time scales that would be required to obtain an equilibrium distribution in a simulation are too large to be accessible currently.

Nevertheless, between 0.57 and 0.81 nm^2/molecule (LC–LE coexistence region), increasing the system size and the time scale simulated [Fig. 2(b), *large circles*] does not change the calculated methyl and methylene signals significantly. The shape of the signal calculated as a function of the area density agrees also well with the experiment [Fig. 2(b) *crosses*]. This indicates that in this region the signal is relatively insensitive to the lateral heterogeneity of the system.

In contrast, once the monolayer has ruptured ($A > 1.05\,nm^2$) the degree of ordering is strongly dependent on the size of the system simulated. The low degree of order of the lipids in the L–G interface and the overestimation of the number of lipids in the L–G interface due to the artificially small pores in the simulations leads to a significant *under*estimation of the overall lipid order in the comparatively small systems simulated. As a consequence, the sharp drop in the CH_2 signal around 1.10 nm^2/molecule cannot be reproduced in the simulations of the small monolayer patches. Increasing the system size, however, results in a significant decrease in the CH_2 signal at 1.14 nm^2/molecule [Fig. 2(b) *large circles*]. This correlates with an increase in lipid order [Fig. 6(b) *large symbols*] and a decrease in the number of gauche defects. For larger systems with fewer but larger pores a further decrease of the CH_2 signal is expected. Thus we believe that the onset of pore formation may well account for the sudden decrease in signal observed experimentally.

The rupture of the larger monolayer occurs at a smaller molecular area [0.97 nm^2, Fig. 9(a)] than in the smaller system. The exact point of rupture is very sensitive to details of the force field[31] and the small discrepancy between the experiment and the simulations in respect to the area per molecule at which the transition occurs is not significant. Due to the increased order, the methyl signal at 0.97 and 1.14 nm^2/molecule also increases with increasing system size. In the experiments no methyl signal was detected at these areas.[3]

SUMMARY AND CONCLUSIONS

In this work we have examined the phase behavior of DPPC monolayers at an air–water interface at varying area densities. Molecular-dynamics simulations suggest that the nature of a sharp transition in the order of the lipid chains at 1.10 nm^2/molecule recently detected by vibrational sum-frequency generation (VSFG) spectra is associated with the onset of the gas–liquid coexistence region. Despite artifacts due to the finite size of the system, the shape of the expected signal from the methylene groups as a function of area density calculated from the simulations agrees well with the experimental data. At 0.57 nm^2/molecule the lateral separation of highly ordered and disordered lipids is observed, indicating the co-existence of the liquid condensed (LC) and the liquid expanded (LE) phase. As the area is expanded further, the proportion of the LC phase decreases. Expanding the monolayer beyond 0.80 nm^2/molecule, however, induces the transient formation of small pores. Around 1.0 nm^2 the monolayer ruptures, marking the onset of the liquid–gas (L–G) coexistence region. The rupture of the monolayer is associated with an increase in the overall lipid order due to increased local packing in the liquid domains. Failure to detect pores by fluorescence microscopy suggests that at the rupture point pores have an equilibrium size smaller than ~500 nm in diameter. Although the present study was performed for DPPC monolayers at an air–water interface, we expect that the rupture of a lipid or surfactant monolayer will lead to a sharp increase of alkyl chain order in most systems. This increase of alkyl chain order is expected to be detectable by VSFG measurements which thus may represent a sensitive means to determine the onset of the L–G coexistence region for such systems.

In the simulations the water level is elevated inside the pores. This was facilitated by a lifting of lipid headgroups. Although at the pore boundaries the lipid tails are highly disordered, the overall lipid order is higher in the ruptured monolayer than in the fully expanded monolayer. This may indicate that in the liquid–gas coexistence region LC domains form in the liquid phase. This challenges the assumption that the liquid phase coexisting with the gas phase is purely the LE phase.[9]

Finally our work demonstrates that it is possible to simulate the onset of phase separation in gel- and fluidlike domains in lipid systems at an atomic level, opening the possibility to study such phenomenon in unprecedented detail.

ACKNOWLEDGMENTS

The authors thank H. Möhwald for useful discussions and A. H. de Vries for providing the equilibrated DPPC bilayer. This project was funded by the from Molecule tot Cell program of the Netherlands Organization for Scientific Research (NWO), Grant No. 80547091.

[1] V. M. Kaganer, H. Möhwald, and P. Dutta, Rev. Mod. Phys. **71**, 779 (1999).
[2] P. Dynarowicz-Latka, A. Dhanabalan, and O. N. Oliveira, Adv. Colloid Interface Sci. **91**, 221 (2001).
[3] S. Roke, J. Schins, M. Müller, and M. Bonn, Phys. Rev. Lett. **90**, 128101 (2003).
[4] E. M. Scarpelli, Anat. Rec. **251**, 491 (1998).
[5] J. A. Zasadzinski, J. Ding, H. E. Warriner, F. Bringezu, and A. J. Waring, Curr. Opin. Colloid Interface Sci. **6**, 506 (2001).
[6] O. Albrecht, H. Gruler, and E. Sackmann, J. Phys. (Paris) **39**, 301 (1978).
[7] N. Denicourt, P. Tancrede, and J. Teissie, Biophys. Chem. **49**, 153 (1994).
[8] R. Veldhuizen, K. Nag, S. Orgeig, and F. Possmayer, Biochim. Biophys. Acta **1408**, 90 (1998).
[9] M. Lösche, E. Sackmann, and H. Möhwald, Ber. Bunsen-ges. Phys. Chem. **87**, 848 (1983).
[10] S. Wurlitzer, T. M. Fischer, and H. Schmiedel, J. Chem. Phys. **116**, 10877 (2002).
[11] S. Siegel and D. Vollhardt, Colloids Surf., A **116**, 195 (1996).
[12] H. Möhwald (private communication).
[13] A. G. Lambert, *Sum frequency spectroscopy of adsorption on hydrophilic mica substrates*, Ph.D. thesis, University of Cambridge (2001).
[14] Y. R. Shen, Nature (London) **337**, 519 (1989).
[15] I. Langmuir, J. Am. Chem. Soc. **39**, 1848 (1917).
[16] W. F. van Gunsteren and H. J. C. Berendsen, Angew. Chem., Int. Ed. Engl. **29**, 992 (1990).
[17] E. Okamura, N. Fukushima, and S. Hayashi, Langmuir **15**, 3589 (1999).
[18] M. S. Tomassone, A. Couzis, C. M. Maldarelli, J. R. Banavar, and J. Koplik, J. Chem. Phys. **115**, 8634 (2001).
[19] Y. N. Kaznessis, S. T. Kim, and R. G. Larson, Biophys. J. **82**, 1731 (2002).
[20] Y. N. Kaznessis, S. Kim, and R. G. Larson, J. Mol. Biol. **322**, 569 (2002).
[21] H. J. C. Berendsen, D. van der Spoel, and R. van Drunen, Comput. Phys. Commun. **91**, 43 (1995).
[22] O. Berger, O. Edholm, and F. Jähnig, Biophys. J. **72**, 2002 (1997).
[23] J. Hermans, H. J. C. Berendsen, W. F. van Gunsteren, and J. P. M. Postma, Biopolymers **23**, 1513 (1984).
[24] B. Hess, H. Bekker, H. J. C. Berendsen, and J. G. E. M. Fraaije, J. Comput. Chem. **18**, 1463 (1997).
[25] S. Miyamoto and P. A. Kollman, J. Comput. Chem. **13**, 952 (1992).
[26] K. A. Feenstra, B. Hess, and H. J. C. Berendsen, J. Comput. Chem. **20**, 786 (1999).
[27] H. J. C. Berendsen, J. P. M. Postma, W. F. van Gunsteren, A. DiNola, and J. R. Haak, J. Chem. Phys. **81**, 3684 (1984).
[28] I. G. Tironi, R. Sperb, P. E. Smith, and W. F. van Gunsteren, J. Chem. Phys. **102**, 5451 (1995).
[29] C. Anezo, A. H. de Vries, H. D. Holtje, D. P. Tieleman, and S. J. Marrink, J. Phys. Chem. B **107**, 9424 (2003).
[30] X. Zhuang, P. B. Miranda, D. Kim, and Y. R. Shen, Phys. Rev. B **59**, 12632 (1999).
[31] H. Leontiadou, A. E. Mark, and S. J. Marrink, Biophys. J. **86**, 2156 (2004).